*Research Article*

# Water Pollution Control and Treatment Based on Quantum Dot Chemical and Biological High-Sensitivity Sensing

**Guihua Zheng[ID], Shiyao Li, Ting Zhang, Feiyun Zhu, Jing Sun, Shuangjiang Li, and Linfeng You**

*School of Materials and Environmental Engineering, Chengdu Technological University, Chengdu, 611730 Sichuang, China*

Correspondence should be addressed to Guihua Zheng; 20143157@stu.nun.edu.cn

Inorganic pollutants in water can have an important impact on ecosystems and human health, so the development of rapid and sensitive detection methods for typical inorganic pollutants in water samples is important for understanding the pollution status of the water environment, as well as water pollution prevention and protection of drinking water safety. Fluorescence sensing technology has the advantages of fast response, high sensitivity, simple operation, and low cost but still has the problems of low quantum yield, cumbersome construction process, and limited practical applications. Based on the excellent fluorescence properties, a series of fluorescence sensing was constructed for the rapid, highly sensitive, and selective detection of various typical inorganic pollutants in water. And the related fluorescence sensing mechanism was investigated in this paper. In this paper, nitrogen/sulfur codoped carbon quantum dots (N, S-CQDs) were prepared for the sensitive and selective detection of sulfide and ferric ion. The blue fluorescent N, S-CQDs were prepared by a one-step hydrothermal method using ammonium citrate and L-cysteine as raw materials, which have excitation wavelength dependence and fluorescence quantum yield of 16.1% for the selective detection of sulfides with a detection limit (S/N = 3) of 11.0 nM (about 0.35 $\mu$g/L). CQDs with significantly higher fluorescence quantum yields (69%) and no excitation dependence were prepared when citric acid was used instead of ammonium citrate and were used for the selective detection of ferric ion with a detection limit of 14.0 nM (~0.8 $\mu$g/L). The method has been successfully applied to the determination of total phosphorus in surface water and human urine, and the fluorescence color change of the dual-emission sensing can be used for the naked-eye identification and semiquantitative detection of phosphate.

## 1. Introduction

In recent years, with the continuous development of other related disciplines, fluorescence analysis has been greatly developed in terms of theoretical research and analytical application; a variety of fluorescence analysis methods such as synchronous fluorescence, fluorescence polarization, fluorescence lifetime, time-resolved fluorescence, fluorescence immunoassay, and fluorescence microscopy imaging have been developed successively; and multifunctional fluorescence detection instruments have been introduced one after another [1]. Fluorescence analysis has been developed in the direction of rapid, sensitive, efficient, real-time, and in situ and has become an important analytical tool in food safety analysis, environmental monitoring, pharmaceutical analy-

sis, and clinical diagnosis [2]. Fluorophores and recognition groups are the two main components of fluorescence sensing. The recognition groups can specifically bind or interact with the target analytes, causing fluorescence changes in the fluorophores and outputting fluorescence signals through the fluorescence spectrometer to achieve the determination of the target analytes; therefore, fluorescence sensing modified by specific recognition groups can selectively identify the target analytes and thus achieve the qualitative and quantitative analysis of the target analytes in complex samples [3]. Therefore, the fluorescence sensing modified with specific recognition groups can selectively identify the target analytes, thus enabling qualitative and quantitative analysis of the target analytes in complex samples [4]. Photoinduced electron transfer, a process in which the fluorescence is

quenched by electron transfer between the energy orbitals of the excited state and the electron donor after the electron donor is excited by light, is widely used in the design of metal ion fluorescence sensing [5]. The fluorescence sensing based on PET mechanism usually consists of three parts: fluorophore (fluorophore), recognition group (receptor), and linker arm (spacer), which mostly contain conjugated structures (naphthalene, pyrene, and anthracene), are responsible for absorbing light energy and emitting fluorescence, and are electron acceptors; the recognition group generally contains N, O, S, and other heteroatoms, which can specifically bind to the target [6]. The linker arm is used for the connection between the fluorophore and the recognition group [7].

The design, synthesis, and modification of fluorescent materials determine the structural composition, fluorescence stability, and fluorescence sensing performance of the target. In order to meet the evolving needs of fluorescence sensing, researchers have developed a series of different types of fluorescent sensing materials based on physical, chemical, and biological principles and nanotechnology, including organic dyes, fluorescent proteins, nanofluorescent sensing, and complex fluorescent sensing. Carbon quantum dots (CQDs), as a new member of the carbon nanomaterial family, have good water solubility, photobleaching resistance, biocompatibility, low biotoxicity, simple synthesis method, green, and low cost, making them an excellent alternative to traditional organic dyes and semiconductor quantum dots [8]. As a long fluorescence lifetime material, rare-earth ion complexes can not only reduce background fluorescence interference and improve detection sensitivity and accuracy but also be used for time-resolved fluorescence determination. Carbon quantum dots are nanoparticles with sizes between 1 and 10 nm. In 2004, researchers discovered the first fluorescent zero-dimensional carbon nanomaterials in the isolation and purification of single-walled carbon nanotubes. In 2006, researchers prepared carbon nanomaterials with high fluorescence quantum yields by combining laser exfoliation of graphite and surface passivation, which led to the concept of "carbon quantum dots." The concept of "carbon quantum dots" has received a lot of attention from researchers and has led to a boom in research on carbon quantum dots. Due to their excellent nanoscale properties, fluorescence properties, biocompatibility, and optoelectronic properties, carbon quantum dots are widely used in many fields such as analytical detection, fluorescence imaging, drug delivery and therapy, catalysis, and optical devices [9]. The results of many studies have shown that carbon quantum dots obtained by different preparation methods contain sp3 hybridized carbon (diamond structure) in addition to sp2 hybridized carbon (graphite structure), and the luminescence of carbon quantum dots is related to both hybridization methods. Under UV light irradiation, carbon quantum dots can exhibit different colors of fluorescence, but the detailed mechanism of fluorescence generation and the exact origin of the differences in fluorescence properties of carbon quantum dots are still controversial [10]. The present results suggest that the luminescence mechanism of carbon quantum dots may involve quantum effects, surface emission traps, exciton radiation recombination, and other factors. Some

researchers believe that the size can significantly affect the luminescence effect of carbon quantum dots [11]. Due to the uncontrolled synthesis process of carbon quantum dots, carbon quantum dots have different particle size distributions and show their emission wavelengths depending on excitation wavelengths, and their fluorescence spectra extend from the visible region to the near-infrared region gradually; when the size distribution of carbon quantum dots is uniform, they show emission wavelengths that do not depend on excitation wavelengths. The researchers prepared the carbon quantum dots by the alkali-assisted electrochemical method, which provided the basis for the quantum effect and the size-dependent fluorescence properties [12]. To further demonstrate that the fluorescence of carbon quantum dots originates from the quantum effect, they then investigated the relationship between fluorescence and nanometer size through theoretical calculations.

From the above research progress, it can be seen that the fluorescence sensing methods based on fluorescent carbon quantum dots and rare-earth ion complexes and their applications have been significantly progressed and at the same time provide opportunities for the construction of rapid, sensitive, and selective detection methods for inorganic pollutants in water bodies. This paper presents new techniques and methods for fluorescence sensing based on carbon quantum dots and ionic complexes and designs several aqueous-phase stable and environment-friendly single- and dual-emission fluorescence sensing methods to achieve single-target detection to simultaneous detection of multiple targets and to be used for rapid, highly sensitive, and selective analysis and determination of various typical inorganic pollutants in water. In this paper, we prepare fluorescent carbon quantum dots (N, S-CQDs) codoped with nitrogen/sulfur and investigate the relationship between their fluorescence properties and structure and the raw materials used for their preparation; improve the fluorescence quantum yield of N, S-CQDs; improve their surface chemistry and fluorescence properties, investigate the analytical performance of N, S-CQDs for the detection of sulfide and ferric ion in water samples; and reveal the response mechanism. In order to address the above mentioned problems, this work is aimed at synthesizing and constructing functional fluorescent carbon quantum points and rare-earth dione complexes and at examining the relationship between carbon quantum points through two-element dosing and the structure and properties of their synthetic materials. By studying the mechanism of interaction between rare-earth diones and organic ligands or carbon quantum points, we will develop a new method to construct stable and environmentally friendly rare-earth dione complexes in the aqueous phase. Based on fluorescence sensory sensors, we are developing new methods for the construction of carbon quantum points and rare-earth dione complexes.

## 2. Related Work

Rare-earth elements include scandium, yttrium, and 15 lanthanides in the third subgroup of the periodic table, which are known as "industrial vitamins" due to their unique

electron layer structure and physical and chemical properties, exhibiting special properties in light, electricity, and magnetism. Rare-earth elements often exist in the form of trivalent ions, which have an electron arrangement of [Xe]4f0-14, with 5s25p6 electron orbitals that are completely filled with electrons and 4f electron orbitals that are not filled with electrons. Since the absorption and emission of rare-earth ions depend mainly on the leap between the 4f-4f energy levels in the inner layer, the f-f leap of rare-earth ions is a forbidden leap according to Laporte's rule, so the molar absorption coefficient of rare-earth ions for UV-visible light is small, and the direct absorption of light is weak, which leads to very weak fluorescence of rare-earth ions and limits the promotion of its application [13]. Weissman first discovered that the complexes formed by the combination of $\beta$-diketones and Eu could emit the strong characteristic fluorescence of Eu under UV excitation, and since then, the research on the rare-earth ion complexes has attracted a lot of attention from researchers. According to Lewis' acid-base theory and Pearson's soft and hard acid-base rules, rare-earth ions belong to hard acids and can combine with organic ligands containing hard base atoms such as fluorine, oxygen, and nitrogen to form stable complexes, and the chemical bonding type is mainly ionic. The large ionic radius and bonding characteristics of rare-earth ions determine their high coordination number, and rare-earth ion complexes with coordination numbers of 6-10 can be formed when the relative sizes of organic ligands and rare-earth ions permit [14]. The weak direct light absorption ability of rare-earth ions leads to their weak fluorescence, and when combined with organic ligands, rare-earth ion complexes are formed. Since organic ligands have strong absorption of UV light, they can transfer the absorbed energy to the central rare-earth ion in the form of radiation-free, sensitized rare-earth ion luminescence; this use of organic ligands as absorption antenna to eliminate rare-earth ion f-f leap ban resistance, and then enhancing the process of rare-earth ion characteristic fluorescence is called the antenna effect. The antenna effect of rare-earth ion complexes includes the absorption of energy by organic ligands, the transfer of ligand energy to rare-earth ions, and the luminescence of rare-earth ions [15].

The absorption of UV light by ligands is a prerequisite for the luminescence of rare-earth ion complexes; therefore, a ligand with a high molar absorption coefficient is the key to improve the fluorescence intensity of rare-earth ions. The presence of rigid structures and electron-rich conjugation systems in organic ligands helps to improve the absorption of UV light. The larger the conjugation system of the ligand, the stronger the absorption of UV light and the easier the $\pi$-$\pi*$ leap occurs. In addition, when the degree of conjugation of rare-earth ion complexes is greater, the greater the degree of rigidity, the more stable their structure, the better the mobility of electrons, the less energy loss in the luminescence process, and the higher the luminescence efficiency [16]. Dexter's solid-state sensitized luminescence theory shows that the energy conversion efficiency depends on the match between the triplet energy level of the ligand and the vibrational energy level of the excited state of the rare-earth ion, and in general, the triplet energy level of the ligand is 2000-4500 cm$^{-1}$ higher than the lowest excited state energy level of the rare-earth ion. In general, the triplet energy level of the ligand is 2000 cm$^{-1}$ higher than the lowest excited state energy level of the rare-earth ion, and too large or too small an energy level difference will affect the energy transfer process, which in turn affects the electron leap efficiency and fluorescence quantum yield of the rare-earth ion [17].

From the luminescence mechanism, it can be seen that the ligand is responsible for absorbing the excitation light and then transferring the energy to the rare-earth ion, which absorbs the energy and jumps to the excited state and then releases the photon when it returns to the ground state from the excited state and emits its characteristic fluorescence. Since the characteristic fluorescence peaks of rare earths are narrow (the half-peak width is generally 10-15 nm), the emission peaks of different rare-earth ions do not easily overlap, so multiemission fluorescence complexes can be designed by doping rare-earth ions with different emission centers to achieve ratiometric fluorescence detection or multitarget detection [18]. The f-f leap within the 4f electron orbital of the complex is effectively shielded by the outer 5s and 5p orbitals, resulting in the 4f orbital not being directly involved in the bonding of chemical bonds, so that the fluorescence emission of the rare-earth center ions is almost unaffected by the external environment as well as the coordination field, thus presenting a sharp linear emission spectrum with correspondingly high purity of luminescence color for easy discrimination [19]. In summary, the selection of organic ligands with high molar absorption coefficients, good energy level matching with rare-earth ions, and conjugated structures is the key to improve the luminescence efficiency of rare-earth ion complexes, while the reduction of the coordination number of water molecules also contributes to the improvement of fluorescence yields. Since the excited state energy levels of Eu and Tb$^{3+}$ are better matched with the excited triplet state energy levels of organic ligands, and the red and the green characteristic fluorescence of both are in the visible region, belonging to the triplet primary colors with high emission intensity and good luminescence monochromacy, they have great potential for applications in sensing analysis, bioimaging, and optoelectronic materials [20].

## 3. Selective Detection of Contaminants by Codoped Carbon Quantum Dots

*3.1. Carbon Quantum Dot Preparation Process.* Harmful ion pollution in environmental waters poses a serious threat to human health and is of increasing concern. Among them, Hg$^{2+}$ is extremely harmful to human body because of its easy accumulation in organisms and strong interaction with sulfhydryl groups of proteins. Sulfides have received much attention because of their important role in life sciences and natural environment. Industrial and domestic wastewater discharges are the main sources of sulfides, and anaerobic microorganisms in water bodies can also produce sulfides by reducing sulfates. Sulfides can combine with protons to form HS$^-$ or H$_2$S, protonated sulfides are more toxic to organisms,

and their abnormal levels can lead to a variety of diseases, including cirrhosis, Alzheimer's disease, and Down syndrome. As a toxic pollutant, sulfide has been listed as an important environmental indicator for springs, surface water, and wastewater. And achieving rapid and sensitive detection of ferric ion is important for studying iron metabolism and anemia diagnosis. In recent years, fluorescence sensing has received much attention because of its easy operation, high sensitivity, and low cost, and the fluorescence sensing method based on nanomaterials is simpler and more effective, and several types of semiconductor quantum dots have been used for colorimetric or fluorescence detection of sulfides, as shown in Figure 1. Fluorescent carbon quantum dots (CQDs) have attracted much attention because of their excellent optical properties, good biocompatibility, low cost, low toxicity, and chemical stability, and compared with semiconductor quantum dots, element-doped carbon quantum dots have more excellent performance, and some fluorescent carbon quantum dots have been used for the detection of sulfides and ferric ion, but most of the methods have low detection sensitivity and. However, most of the methods have low sensitivity and need to be further improved. The N, S-CQDs were prepared by a one-step hydrothermal method as follows: a certain weight ratio (2/1) of ammonium citrate (AC) and L-cysteine (L-Cys) was dissolved in 5.0 mL of ultrapure water, and then, the mixture was transferred to a 100 mL polytetrafluoroethylene reactor, heated at 200°C for 5 h, and then cooled naturally to room temperature. Then, the reaction product was filtered with a 0.22 $\mu$m microporous membrane to remove the insoluble material, and the N, S-CQD solution was purified by dialysis using a dialysis bag with a MWCO of 1000 Da, and the purified bright brown N, S-CQDs solution was dried overnight at 50°C under vacuum to obtain a solid powder. The powder was redispersed into high purity water to obtain N, S-CQD stock solution (2.0 g L$^{-1}$) and placed in a refrigerator at 4°C for use.

The cytotoxicity of N, S-CQDs was determined by the standard MTT method as follows: 100 $\mu$L of HepG$_2$ cells was inoculated in a 96-well plate at a density of $1.0 \times 105$ cell mL$^{-1}$; the cells were incubated in a constant-temperature incubator at 37°C with 5% CO$_2$ for 24 h. Five wells were selected as blanks, and the medium was removed from the remaining wells. After 24 h incubation in a constant temperature incubator with 5% CO$_2$ at 37°C, five wells were selected as blanks, the medium was removed from the remaining wells, and the N, S-CQD solution (N, S-CQDs dissolved in DMEM medium containing 10% FBS) at different concentrations (0, 100, 150, 200, and 300 mg L$^{-1}$) was added, and incubation was continued for 24 h. Afterwards, all wells were aspirated and washed three times with PBS solution (pH = 7.4). After that, all wells were aspirated and washed three times with PBS solution (pH = 7.4), 20 $\mu$L of MTT solution (5.0 g L$^{-1}$) was added to each well, and the cells were incubated in the incubator for 4 h to form formazan crystals; after that, the medium in all wells was aspirated and 150 $\mu$L of DMSO solution was added to dissolve the formazan crystals; finally, the 96-well plate was placed in an enzyme marker and the formazan crystals in each well

were measured at 570. Finally, the 96-well plates were placed in an enzyme marker, and the optical density (OD) of the mixed solution in each well was measured at 570 nm (five times in parallel); the cell survival rate was calculated using the following formula: viability (%) = OD of experimental group/OD of control group × %. In a 10.0 mL colorimetric tube, 100 $\mu$L of phosphate buffer solution (1.0 M, pH = 6.0), 100 $\mu$L of N, S-CQDs (2.0 g L$^{-1}$), and 30 $\mu$L of Hg$^{2+}$ solution (10.0 m M) were added sequentially, and then, a certain concentration of sulfide (0.1-20.0 $\mu$M) was added after the reaction was left for 5 min. After 5 min of reaction, a certain concentration of sulfide (0.1-20.0 $\mu$M) was added; finally, the mixture was diluted to 10.0 mL with ultrapure water, mixed thoroughly, and allowed to stand for 30 min before measurement. All samples were placed in a 1 cm quartz cuvette, and the fluorescence intensity at 435 nm was measured at a 355 nm excitation wavelength with excitation and emission slits set to 10 nm. In the selectivity test, other cations, anions, or FA was used instead of sulfide, and the same determination method was used.

### 3.2. Cytotoxicity Experiments of Carbon Quantum Dots. As shown in Figure 2, the fluorescent carbon quantum dots (N, S-CQDs) codoped with nitrogen/sulfur were prepared by a one-step hydrothermal method using ammonium citrate as the carbon/nitrogen source and L-cysteine as the nitrogen/sulfur source. The fluorescence spectra and UV absorption spectra are shown in Figure 3. The results show that the N, S-CQD solution has bright blue fluorescence at 435 nm and strong UV absorption at around 330 nm. When Hg$^{2+}$ was added to the N, S-CQD solution, the N, S-CQDs accumulated and underwent charge transfer to Hg$^{2+}$, and their fluorescence was quenched and the UV absorption peak at 330 nm was also reduced. When sulfide was added to the N, S-CQD-Hg$^{2+}$ system, the fluorescence of the system was restored because the sulfide could effectively bind to Hg$^{2+}$, thus removing Hg$^{2+}$ from the surface of the N, S-CQDs. The fluorescence of N, S-CQDs was significantly quenched by the addition of Hg$^{2+}$, and the fluorescence of the system was restored by the subsequent addition of sulfide, based on which we proposed a fluorescence "turn-off-on" sensing method based on N, S-CQDs for sulfide analysis. We propose a N, S-CQD fluorescence "turn-off-on" sensing method for sulfide analysis. Weigh 20 mg of Eu-CP powder and disperse it in 100 mL of aminoacetic acid buffer solution (20 mM, pH 6.5) and sonicate for 5 min to obtain a homogeneous dispersion of Eu-CPs (0.2 g L$^{-1}$). In a 10.0 mL cuvette, 5.0 mL of Eu-CP solution and 1.0 mL of N, S-CQD solution (0.1 g-L-1) were added sequentially, followed by a certain concentration of phosphate (0.5-200.0 $\mu$mol L$^{-1}$) or ferric ion (0.5200.0 $\mu$mol L$^{-1}$) standard solution.

The results showed that the fluorescence intensity of the N, S-CQDs prepared under different WAC/WL-Cys conditions was significantly different; when the WAC/WL-Cys was 2:1, the fluorescence of N, S-CQDs was the strongest and the response to Hg$^{2+}$ or sulfide was significant, so the mass ratio of 2/1 ammonium citrate and L-cysteine was selected for the preparation of N, S-CQDs. It was found that the heating temperature and time did not significantly affect the
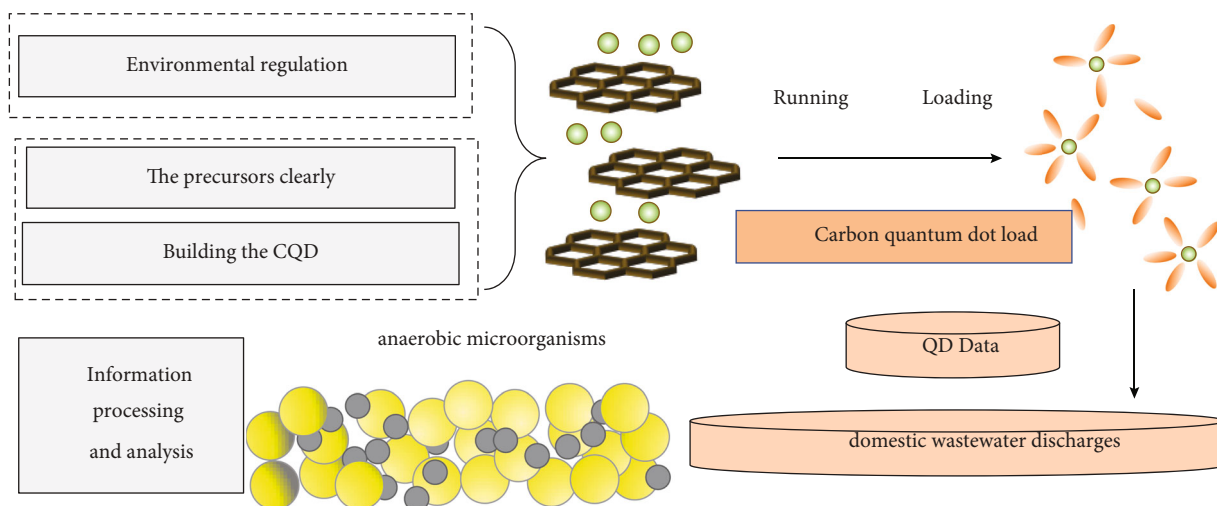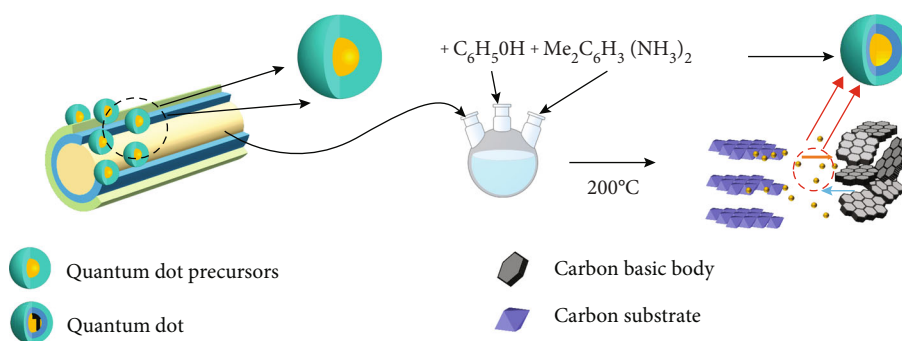
FIGURE 1: Fluorescence detection process.



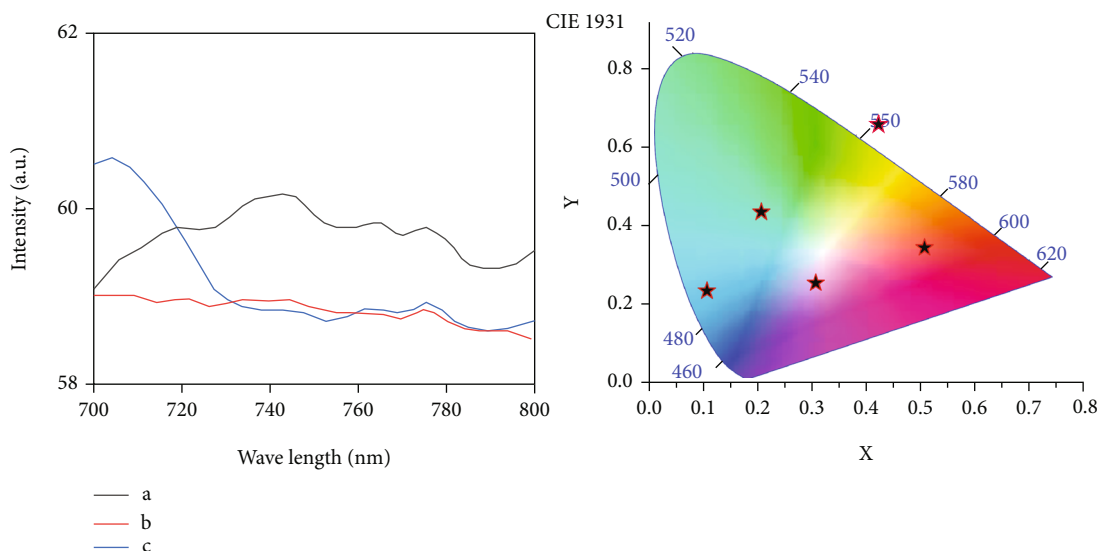FIGURE 2: Schematic diagram of CQDs for $Hg^{2+}$ and sulfide detection.



FIGURE 3: Fluorescence spectra and UV absorption spectra of sulfides.

fluorescence properties of N, S-CQDs when the carbon quantum dots were prepared by the hydrothermal method, so the heating temperature of 180°C and the reaction time of 12 h were chosen as the preparation conditions of N, S-CQDs.

3.3. *Design of Fluorescence Sensing.* The above mixed solution was placed in a 1 cm cuvette, and the emission spectra were scanned in the wavelength range of 370-750 nm with the excitation wavelength of 285 nm. The linear relationship

between the fluorescence intensity ratio at 617 nm and 420 nm (I617/I420) and phosphate concentration was used for the quantitative analysis of phosphate, and the linear relationship between fluorescence intensity at 420 nm and ferric ion concentration was used for the quantitative analysis of ferric ion. In the selectivity test, the phosphate and ferric ion were replaced by other possible interfering substances and determined analytically using the same determination method described above. The red fluorescent Eu-CPs were rapidly prepared under ambient aqueous phase conditions, and the Eu-CPs could fluorescently respond to ferric ion and phosphate at the same time, as shown in Figure 4. The response results showed that the blue fluorescent N, S-CODs obtained by the one-step hydrothermal method could selectively recognize ferric ion. The N, S-CQD/Eu-CP dual-emission fluorescence sensing system was constructed by mixing the N, S-CCOD and Eu-CP aqueous solution in a certain ratio, which has two emission peaks at 420 nm and 617 nm, indicating the characteristic fluorescence peaks of N, S-CCODs and Eu-CPs, respectively. When phosphate was added to the sensing system, the fluorescence at 617 nm was significantly quenched, and the fluorescence intensity at 420 nm remained stable, which could be used as the reference fluorescence, and the linear relationship between the ratio of the fluorescence intensity at 617 nm and 420 nm (I617/I420) and the concentration of phosphate was used for the determination of the phosphate ratio. The naked-eye identification of Pi was achieved by the fluorescence color change of this dual-emission system. In addition, since the fluorescence at 420 nm is selective for ferric ion, it can be used for the analytical determination of ferric ion. Therefore, the dual-emission fluorescence sensing of N, S-CQDs/Eu-CPs can realize the simultaneous detection of phosphate and ferric ion.

Silver, as a precious metal, is a cost-effective metal catalyst with a wide range of applications in photography, electronics, optics, and medicine. Silver ions ($Ag^+$) in industrial wastewater have been classified as a toxic metal contaminant in ambient air, water, soil, and even food. Due to their antimicrobial activity, $Ag^+$ can be highly toxic to many environmentally harmless or environmentally beneficial bacteria. In addition, they can inactivate sulfhydryl enzymes and bind to various metabolite groups such as imidazole, amine, and carboxyl groups, which eventually accumulate in the human body. Therefore, it is important to establish a rapid, simple, and efficient method for the sensitive and selective determination of $Ag^+$ in environmental media. Currently, $Ag^+$ detection techniques based on electrochemical methods, colorimetric methods, and fluorescence analysis have been widely reported, and fluorescence analysis has the advantages of high sensitivity, rapidity, and simplicity, which is a more ideal detection method. In recent years, due to the development of nanotechnology, the application of quantum dots in fluorescence analysis has received more and more attention. Functionalized quantum dots for sensitive and selective detection of $Ag^+$ are usually modified with stabilizers such as small molecules containing sulfhydryl groups, proteins, and DNA. However, the reported sensitivity of functionalized quantum dots for
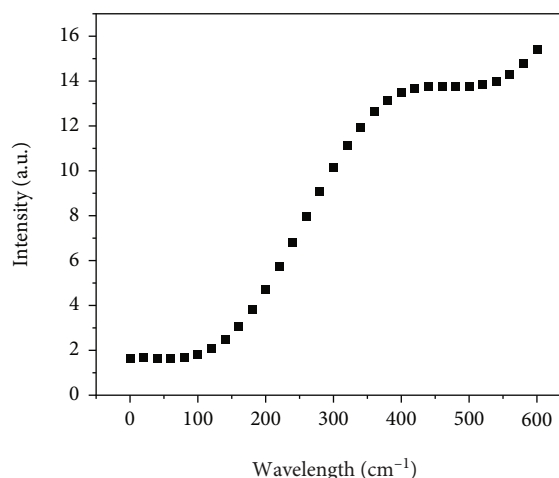


FIGURE 4: Fluorescence response spectra of phosphate and ferric ion.

$Ag^+$ detection does not meet the requirements of environmental monitoring; moreover, fluorescence analysis based on single-emission fluorescence signal is usually affected by the probe concentration, excitation intensity, and emission light collection efficiency. In contrast, dual-emission fluorescence-based sensing can effectively avoid external environmental interference and help achieve highly sensitive and selective detection of the target. In addition, the target can also induce different colors of fluorescence from dual-emission sensing, and its color change not only facilitates ratiometric analysis but also enables naked-eye visualization of the target.

## 4. Results and Analysis

The fluorescence response of N, S-CQD/Eu-CP dual-emission fluorescence sensing for different concentrations of ferric ion is shown in Figure 5; with the increase of ferric ion concentration, the fluorescence intensity at 420 nm gradually decreases; from it, it can be seen that the fluorescence intensity of N, S-CQDs can be linearly related to the ferric ion concentration when the ferric ion concentration is 0.5-100.0 $\mu$M. The linear equation was $y = -0.56121x + 162.82579$ ($R2 = 0.9948$), and the detection limit of ferric ion was 48.3 nM (about 2.7 $\mu$g/L, and the limit of ferric ion concentration in drinking water was 0.3 mg/L). The selective detection results of ferric ion by N, S-CQD/Eu-CP fluorescence sensing are shown in Figure 5. It can be seen that ferric ion significantly quenched the fluorescence of N, S-CQDs, while other anions and cations did not affect the fluorescence of N, S-CQDs significantly, indicating that the fluorescence sensing can achieve the selective detection of ferric ion.

To evaluate the feasibility of dual-emission fluorescence sensing of N, S-CQDs/Eu-CPs for the analysis of phosphate and ferric ion in real samples, the concentrations of phosphate and ferric ion in lake water were determined by the standard addition method in this study, and the results are shown in Figure 6. The results showed that the sensing
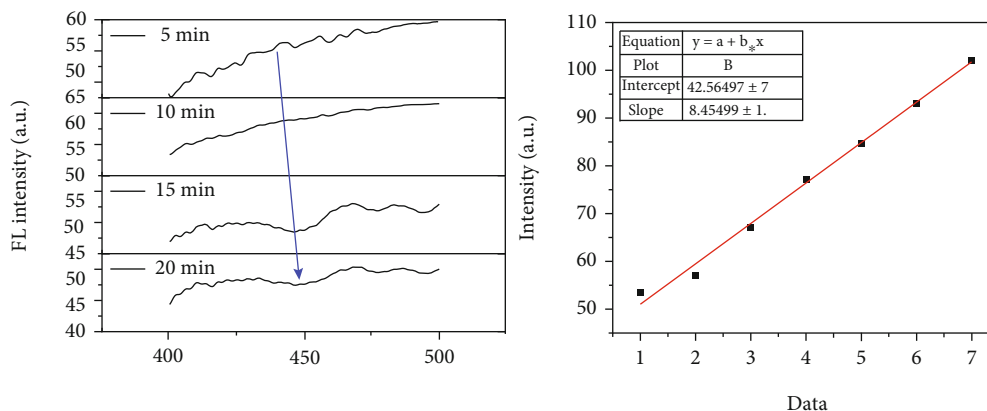
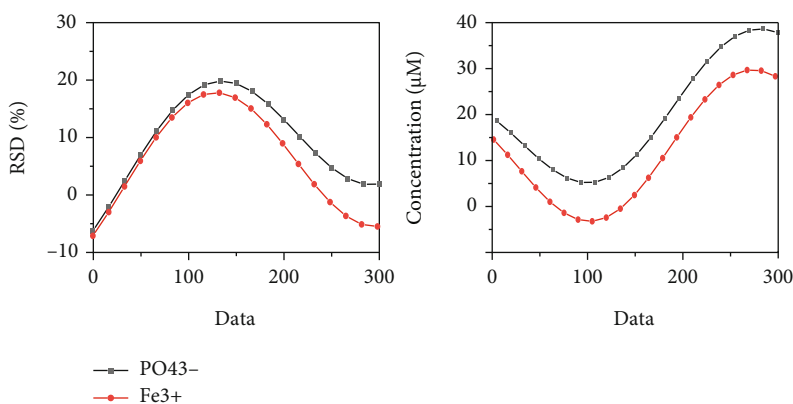FIGURE 5: Fluorescence spectra of ferric ion by the complex sensing system.



FIGURE 6: Simultaneous detection of ferric ion and phosphate in water.

method could detect phosphate and a small amount of ferric ion in the digested lake water, and the recoveries of both were in the range of 95.8-100.3% with the relative standard deviations less than 4.4%. Rare-earth luminescence, especially rare-earth near-infrared luminescence, is of great interest to researchers because of its large Stokes shift, long fluorescence lifetime, sharp emission spectrum, and high color purity for easy discrimination. However, the small molar absorption coefficients of rare-earth ions and the forbidden f-f leap have led to weak luminescence, limiting its application. Coordination polymers (CPs) are new composite materials obtained by coordination of metal ions and organic ligands, which have physical properties such as structural diversity, magnetic properties, luminescence, and porosity. The high affinity between rare-earth ions and hard alkali atoms allows them to combine with organic ligands containing oxygen/nitrogen atoms to obtain lanthanide ion coordination polymers (Ln-CPs), which can emit strong characteristic fluorescence by sensitizing rare-earth ions through the "antenna effect," so Ln-CPs, especially those with Eu and $Tb^{3+}$ as the central bodies, are the new functional luminescent materials. Therefore, Ln-CPs, especially those with Eu and $Tb^{3+}$ as the central bodies, provide an opportunity for the development of new functional luminescent materials. Several Ln-CP luminescent materials have

been reported for nitroaromatic explosives, small molecules, inorganic ions, biomolecules, and pH detection.

In addition, in order to evaluate the practicality of this fluorescence sensing, the phosphate concentration in tap water, lake water, river water, and human urine was measured using this method, and the results were also compared with those determined by the national standard method for the determination of phosphorus molybdenum blue spectrophotometric method, and the results are shown in Figure 7. The results showed that the phosphate concentrations measured by this method were in good agreement with those determined by phosphomolybdenum blue spectrophotometry, indicating that the fluorescence sensing can be used for the selective and accurate detection of phosphate in real samples.

The XRD and fluorescence lifetime characterization results of Eu-CPs before and after the interaction with phosphate are shown in Figure 8. The results showed that the crystal structure of Eu-CPs was completely destroyed after the interaction with phosphate, but the fluorescence lifetime did not change significantly, which was due to the strong binding of oxygen atoms in phosphate with Eu in Eu-CPs, disrupting the binding of Eu to the organic ligand H4btec-ICA, breaking the structure of the complex and blocking the interaction between Eu and H4btec-ICA. This disrupts
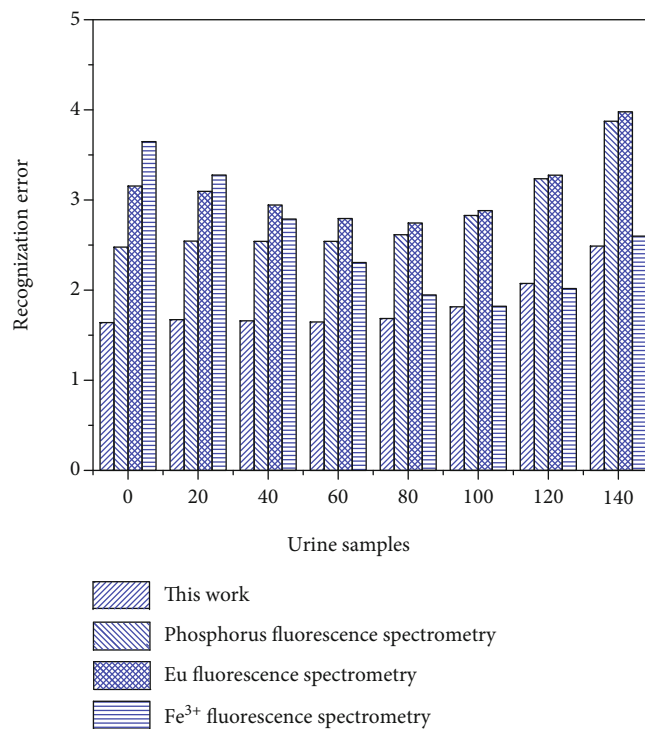
FIGURE 7: Determination of phosphate in water and urine samples by this method and phosphomolybdenum blue spectrophotometry.
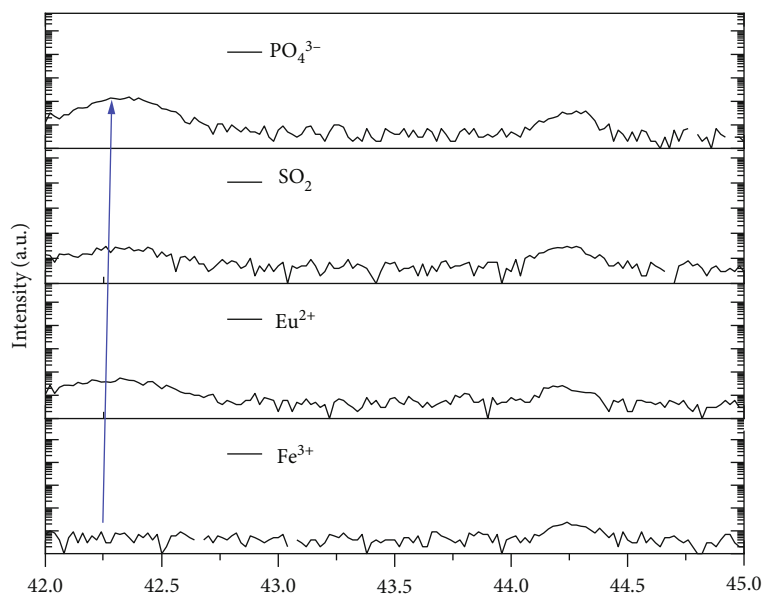


FIGURE 8: Fluorescence lifetime characterization results.

the binding of Eu to the organic ligand H4btec-ICA, disrupting the structure of the complex and blocking the "antenna effect" between H4btec-ICA and Eu, resulting in the static fluorescence quenching of Eu-CPs.

The FT-IR spectrum showed that Eu-CPs/$PO_4^{3-}$ showed a broad P-O peak and the characteristic stretching vibration peak was red-shifted from $1100\,cm^{-1}$ to $1012\,cm^{-1}$ compared to the P-O absorption peak in phosphate. XPS results showed that Eu-CPs had two binding energy peaks at 135.93 and 141.34 eV, which indicated the Eu-O bond formed by the binding of Eu with H4btec-ICA, and in Eu-CPs/$PO_4^{3-}$, the positions of these peaks were shifted to 136.59 eV. In Eu-CPs/$PO_4^{3-}$, these two peak positions are shifted to 136.59 eV and 141.99 eV, which indicate that the oxygen atoms in the phosphate are cobound with the Eu-O cluster in Eu-CPs and effectively inhibit the transition of H4btec-ICA to the Eu-O cluster through the "antenna effect." The energy transfer from H4btec-ICA to the Eu-O

cluster through the "antenna effect" was effectively inhibited, which in turn weakened the characteristic fluorescence of Eu. Nitrite ($NO^{2-}$) is widely used as a food additive and preservative due to its preservative properties. In addition, it is widely used as a dyeing agent, corrosion inhibitor, and chemical fertilizer. However, nitrite pollution caused by agricultural activities and wastewater discharge from the dyeing industry has raised concern, and nitrite has been classified as a typical class of inorganic pollutants in surface water and groundwater. $NO^{2-}$ enters the human body and oxidizes low-iron hemoglobin to high-iron hemoglobin, making it lose its ability to transport oxygen; in addition, it can react with secondary amines to produce N-Nitroso Compounds ⬚NOC⬚. Therefore, $NO^{2-}$ content is considered an important water quality parameter for various water bodies, and the maximum allowable $NO^{2-}$ content in drinking water is set at 3.0 ppm and 1.0 ppm by the World Health Organization (WHO) and the U.S. Department of Environmental Protection (EPA), respectively. Contaminated water is the main way for $NO^{2-}$ and $Hg^{2+}$ to enter the human body. Surface modifications can greatly change the surface state of CQDs, such as the introduction of organic small molecules or metal ions. Rare-earth ions (e.g., $Tb^{3+}$ and Eu) have very low luminescence efficiency on their own, but when specifically bound to ligands, the "antenna effect" sensitizes them to emit strong fluorescence. However, there are no reports of direct energy transfer from CQDs to rare-earth ions and sensitization of their fluorescence.

## 5. Conclusion

The fluorescence analysis method has the characteristics of sensitive response, rapid, easy operation, and low cost, which has a broad application prospect in the detection of environmental pollutants. In this thesis, a series of new fluorescence sensing methods based on fluorescent carbon quantum dots and rare-earth ionic complexes were constructed for the sensitive and selective detection of a variety of typical inorganic pollutants in water samples, and their fluorescence sensing mechanisms were investigated. In this study, Eu-CPs were rapidly prepared under room temperature aqueous phase conditions using Eu as the metal central body and 1,2,4,5-benzenetetracarboxylic acid (H4btec) and imidazole-2-carboxaldehyde (ICA) as the dual organic ligands, which have good fluorescence properties in both aqueous solutions and common organic solvents. By introducing blue fluorescent N, S-CQDs, N, S-CQD/Eu-CP dual-emission fluorescence sensing was constructed; this sensing method can achieve the simultaneous detection of phosphate and ferric ion in water samples with the detection limits of 68.6 nM and 48.3 nM, respectively, and has been successfully applied to the determination of total phosphorus content in surface water and human urine. The method has been successfully applied to the determination of total phosphorus in surface water and human urine, and the fluorescence color change of the dual-emission sensing can be used for the naked-eye identification and semiquantitative detection of phosphate. This study not only developed a rapid and green method for the preparation of Eu-CPs, but also provided new ideas

for the construction of dual-emission fluorescence sensing and the simultaneous detection of multiple target analytes. In this paper, we found that low concentration of sodium dodecylbenzene sulfonate (SDBS) could significantly enhance the resonance energy transfer phenomenon from CIP to Eu and thus constructed a SDBS-sensitized energy transfer CIP-Eu complex fluorescence sensing for the ultrasensitive determination of total phosphorus content in a variety of environmental samples. In the future, the accurate detection of $NO^{2+}$ and $Hg^{2+}$ concentrations in water bodies is particularly important. Fluorescent carbon quantum dots are simple to prepare, highly water soluble, biocompatible, low or nontoxic, easy to surface modify, and have unique optical properties.

## Data Availability

The data used to support the findings of this study are available from the corresponding author upon request.

## Conflicts of Interest

The authors declare that they have no known competing financial interests or personal relationships that could have appeared to influence the work reported in this paper.

## Acknowledgments

## References

[1] N. T. Ngoc Anh, P. Y. Chang, and R. A. Doong, "Sulfur-doped graphene quantum dot-based paper sensor for highly sensitive and selective detection of 4-nitrophenol in contaminated water and wastewater," *RSC advances*, vol. 9, no. 46, pp. 26588–26597, 2019.

[2] N. K. Botcha, R. R. Gutha, S. M. Sadeghi, and A. Mukherjee, "Synthesis of water-soluble Ni (II) complexes and their role in photo-induced electron transfer with MPA-CdTe quantum dots," *Photosynthesis research*, vol. 143, no. 2, pp. 143–153, 2020.

[3] P. Devi, P. Rajput, A. Thakur, K. H. Kim, and P. Kumar, "Recent advances in carbon quantum dot-based sensing of heavy metals in water," *TrAC Trends in Analytical Chemistry*, vol. 114, pp. 171–195, 2019.

[4] L. S. Lin, T. Huang, J. Song et al., "Synthesis of copper peroxide nanodots for $H_2O_2$ self-supplying chemodynamic therapy," *Journal of the American Chemical Society*, vol. 141, no. 25, pp. 9937–9945, 2019.

[5] M. Mashkani, A. Mehdinia, A. Jabbari, Y. Bide, and M. R. Nabid, "Preconcentration and extraction of lead ions in vegetable and water samples by N-doped carbon quantum dot conjugated with $Fe_3O_4$ as a green and facial adsorbent," *Food chemistry*, vol. 239, pp. 1019–1026, 2018.

[6] Y. Park and B. Park, "Effect of ligand exchange on photocurrent enhancement in cadmium selenide (CdSe) quantum dot water splitting cells," *Results in Physics*, vol. 11, pp. 162–165, 2018.

[7] P. Paydary and P. Larese-Casanova, "Water chemistry influences on long-term dissolution kinetics of Cdse/Zns quantum dots," *Journal of environmental sciences china*, vol. 90, no. 4, pp. 216–233, 2020.

[8] M. Riedel, J. Wersig, A. Ruff, W. Schuhmann, A. Zouni, and F. Lisdat, "AZ-scheme-inspired photobioelectrochemical $H_2O/O_2$ cell with a 1 V open-circuit voltage combining photosystem II and PbS quantum dots," *Angewandte Chemie*, vol. 131, no. 3, pp. 811–815, 2019.

[9] F. Romano, S. Angeloni, G. Morselli et al., "Water-soluble silicon nanocrystals as NIR luminescent probes for time-gated biomedical imaging," *Nanoscale*, vol. 12, no. 14, pp. 7921–7926, 2020.

[10] K. Roy, D. Ghosh, K. R. Sarkar, P. Devi, and P. Kumar, "Chlorophyll (a)/carbon quantum dot bio-nanocomposite activated nano-structured silicon as an efficient photocathode for photoelectrochemical water splitting," *ACS Applied Materials & Interfaces*, vol. 12, no. 33, pp. 37218–37226, 2020.

[11] D. Sahoo, A. Mandal, T. Mitra, K. Chakraborty, M. Bardhan, and A. K. Dasgupta, "Nanosensing of pesticides by zinc oxide quantum dot: an optical and electrochemical approach for the detection of pesticides in water," *Journal of agricultural and food chemistry*, vol. 66, no. 2, pp. 414–423, 2018.

[12] J. Tian, J. Chen, J. Liu, Q. Tian, and P. Chen, "Graphene quantum dot engineered nickel-cobalt phosphide as highly efficient bifunctional catalyst for overall water splitting," *Nano Energy*, vol. 48, pp. 284–291, 2018.

[13] L. Wang and Y. Shi, "Determination of heavy metal ions in seawater by water-soluble quantum dot fluorescence probe," *Journal of Coastal Research*, vol. 98, no. SI, pp. 146–150, 2019.

[14] S. Wang, K. Zhang, Q. Wang et al., "Graphene quantum dot-assisted preparation of water-borne reduced graphene oxide/-polyaniline: from composite powder to layer-by-layer self-assembly film and performance enhancement," *Electrochimica Acta*, vol. 295, pp. 29–38, 2019.

[15] X. Wang, X. Jiang, E. Sharman et al., "Isolating hydrogen from oxygen in photocatalytic water splitting with a carbon-quantum-dot/carbon-nitride hybrid," *Journal of Materials Chemistry A*, vol. 7, no. 11, pp. 6143–6148, 2019.

[16] Y. Yan, D. Zhai, Y. Liu et al., "van der Waals heterojunction between a bottom-up grown doped graphene quantum dot and graphene for photoelectrochemical water splitting," *ACS nano*, vol. 14, no. 1, pp. 1185–1195, 2020.

[17] F. Yang, G. Gao, J. Wang et al., "Chiral $\beta$-HgS quantum dots: aqueous synthesis, optical properties and cytocompatibility," *Journal of colloid and interface science*, vol. 537, pp. 422–430, 2019.

[18] F. Zhang, X. He, P. Ma, Y. Sun, X. Wang, and D. Song, "Rapid aqueous synthesis of CuInS/ZnS quantum dots as sensor probe for alkaline phosphatase detection and targeted imaging in cancer cells," *Talanta*, vol. 189, pp. 411–417, 2018.

[19] D. H. Zhao, X. Q. Yang, X. L. Hou et al., "In situ aqueous synthesis of genetically engineered polypeptide-capped $Ag_2S$ quantum dots for second near-infrared fluorescence/photoacoustic imaging and photothermal therapy," *Journal of Materials Chemistry B*, vol. 7, no. 15, pp. 2484–2492, 2019.

[20] L. Zheng, X. Ye, X. Deng et al., "Black phosphorus quantum dot-sensitized $TiO_2$ nanotube arrays with enriched oxygen vacancies for efficient photoelectrochemical water splitting," *ACS Sustainable Chemistry & Engineering*, vol. 8, no. 42, pp. 15906–15914, 2020.